NANOSYSTEMS: PHYSICS, CHEMISTRY, MATHEMATICS, 2016, 7 (4), P. 711–723

Inhibition of corrosion of mild steel in well water by TiO_2 nanoparticles and an aqueous extract of May flower

P. Nithyadevi[1], R. Joseph Rathish[2], J. Sathiya Bama[1], S. Rajendran[3,*], R. Maria Joany[4], M. Pandiarajan[1], A. Anandan[5]

[1]PG and Research Department of Chemistry, GTN arts College, Dindigul–624005, India

[2]PSNA College of Engineering and Technology, Dinidgul, India

[3]Corrosion Research Centre, Department of Chemistry, RVS Educational Trust's Group of Institutions, Dindigul–624005,India

[4]Sathyabama University, Chennai, India

[5]SKV Higher Sec School, Kandampalayam–637201, India

wmanonithi@gmail.com, *susairajendran@gmail.com

PACS 81.07.-b **DOI 10.17586/2220-8054-2016-7-4-711-723**

Titanium dioxide nanoparticles have been used to control corrosion of mild steel in well water in the absence and presence of an aqueous May flower extract. As the concentration of TiO_2 increases, the inhibition efficiency also increases. 100 ppm of TiO_2 offers 84 % inhibition efficiency. The addition of 10mlof May flower extract enhances the inhibition efficiency to 95 %. Adsorption of TiO_2 on the metal surface follows Langmuir adsorption isotherm. Polarization study reveals that the flower extract-TiO_2 system functions as mixed type of inhibitor, controlling both anodic and cathodic reactions. AC impedance spectra reveal the formation of a protective film on the metal surface. This technology may find application in cooling water systems and concrete technology.

Keywords: corrosion inhibition, nanoparticles, TiO_2, flower extract, *Delonix regia*, adsorption isotherm.

Received: 5 February 2016

Revised: 9 April 2016

1. Introduction

Nanotechnology is an emerging field through which new productions on nano scale can be manufactured. Producing a new generation of textiles which possess antimicrobial properties using nanoparticles has attracted a great deal of attention from both scientists and consumers in recent years [1, 2]. Furthermore, metal nanoparticles show unique properties due to their peculiar electronic configuration, very large surface area and high amount of surface atoms [3]. For instance, metal nanoparticles show a broad absorption band in the visible region of the electromagnetic spectrum [4]. Some amazing properties of metals are used in order to improve the photocatalytic activities of semiconductors, such as TiO_2 and SiO_2, which are among the most efficient ones, resulting in better photocatalytic properties, even under visible rays [5]. Some noble metals, such as Ag [6], Au [7] and Pd [8] have stood the test of time in the field of producing nanocomposites.

Several nanoparticles have been used as corrosion inhibitors. As the particle size decreases, the inhibition efficiency increases because the surface area covered by the nanoparticles on the metal's surface increases. Nano-TiO_2 particles have improved the corrosion resistance of carbon steel [9], Ni-base alloys [10], aluminum surface [11]. A TiO_2 nanoparticle coating has been used to prevent biofilm formation in water and wastewater installations. Copper nanoparticles have improved the corrosion inhibition efficiency of carbon steel. Titanium dioxide (TiO_2) is a very promising metal oxide which has been widely studied as a photocatalyst for organic synthesis [12] and environmental cleaning processes [13]. Recent applications, based on the photocatalysis and photoactivity of TiO_2, include antifouling, antibacterial, deodorizing and self-cleaning functions [14]. In close connection with the developments in academic research, TiO_2 photocatalysis technology has also become more attractive in industrial applications due to its effectiveness, availability, low cost and chemical stability [15].

In this work, TiO_2 nanoparticles were prepared using commercially available titanyl chloride solution and characterization studies by SEM, EDS. The corrosion resistance of mild steel in well water in the presence of titanium dioxide nanoparticles and an aqueous extract of may flower (*Delonix regia)* by weight loss method, polarization study and AC impedance spectra.

2. Experimental methods

2.1. Preparation of TiO_2 nano particles

Stage1: 50 g of titanium tetrachloride of AR grade was chilled in a freezer overnight and placed in a 500 ml flask. To this, 250 ml of deionized ice water was added drop-wise while continuously shaking the flask. The reaction produced an aqueous titanyl chloride.

Stage 2: The titanyl chloride solution was then added dropwise to a solution of 10 ml glycolic acid (Merck, 70 %) in a flask. Deionized water was added dropwise until a total volume of 300 ml was reached, while continuously shaking the flasks.

Stage 3: The precursor solution was then allowed to stand for 15 days at room temperature, until white precipitates formed. The precipitates were filtered using a pressure filtration unit and then washed with water and methanol [16].

2.2. SEM and EDAX spectra

A few drops of the solution containing TiO_2 nanoparticles were dried on a glass plate. The solid mass was used for recording SEM and EDAX. SEM and EDAX were recorded in field Emission Scanning Electron Microscopy (FESEM-SUPRA 5S)-(ARLZEISS, GERMANY).

2.3. Preparation of the specimen

Mild steel specimens (0.026 % S, 0.06 % P, 0.4 % Mn, 0.1 % C, and the rest iron) of the dimensions 1.0 cm $\times$4.0 cm $\times$ 0.2 cm were polished to a mirror finish and degreased with trichloroethylene and used for the weight loss method and surface examination studies.

2.4. Preparation of May flower extract

An aqueous extract of May flower (*Delonix regia*) was prepared by grinding 10 g of flower using sterile mortar and pestle, filtered through three layers of muslin cloth and make up to 100 ml using double distilled water. This aqueous extract was used as corrosion inhibitor. The image of May flower are shown in Fig. 1.

FIG. 1. May flower

2.5. Determination of corrosion rate

The weighed specimens in triplicate were suspended by means of glass hooks in 100 ml of well water containing various concentration of TiO_2 nanoparticles in the presence and absence of may flower extract (FE) for one day. The specimens were taken out, washed in running water, dried, and weighed. From the change in weights of the specimens, corrosion rates were calculated using the following relationship:

$$CR = [(Weight\ loss\ in\ mg)/(Area\ of\ the\ dspecimens\ in\ dm^2 \times Immersion\ periods\ in\ days)]\ mdd. \quad (1)$$

Corrosion inhibition efficiency (IE %) was then calculated using the equation:

$$I.E. = 100[1 - (W_2/W_1)]\%, \quad (2)$$

where, W_1 – corrosion rate in the absence of the inhibitor, and W_2 – corrosion rate in the presence of the inhibitor.

2.6. Potentiodynamic polarization

Polarization studies were carried out in a CHI – Electrochemical workstation with impedance, Model 660A. A three-electrode cell assembly was used. The three electrode assembly is shown in Fig. 2. The working electrode was mild steel. A saturated calomel electrode (SCE) was the reference electrode and platinum was the counter electrode. From the polarization study, corrosion parameters such as corrosion potential (E_{corr}), corrosion current (I_{corr}) and Tafel slopes (anodic = *b*a and cathodic =*b*c) and Linear polarization resistance (*LPR*) were calculated. The scan rate (V/S) was 0.01 and the hold time at (Efcs) was zero and quit time(s) was two.

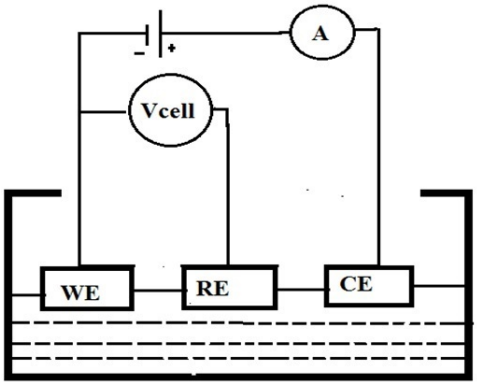

FIG. 2. Circuit diagram of three-electrode cell assembly. WE- working electrode (mild steel), RE-Reference electrode (saturated calomel electrode (SCE)), CE- Counter electrode (platinum)

2.7. AC impedance spectra

AC impedance spectral studies were carried out in a CHI – Electrochemical workstation with impedance, Model 660A. A three-electrode cell assembly was used. The working electrode was mild steel. A saturated calomel electrode (SCE) was the reference electrode and platinum was the counter electrode. The real part (Z') and imaginary part (Z") of the cell impedance were measured in ohms at various frequencies. Values of the charge transfer resistance (R_t) and the double layer capacitance (C_{dl}) were calculated.

3. Results and Discussion

3.1. Characterization of TiO_2 nanoparticles

The TiO_2 nanoparticles have been synthesized. The SEM image of the TiO_2 nanoparticles is shown in Fig. 3. The quantitative results for TiO_2 are shown in Fig. 4.

3.2. Analysis of EDS

EDAX spectrum of TiO_2 nanoparticles is shown in Fig. 5. The data derived from the spectra are given in Table 1. The processing option during recording the spectrum was normalized (all elements were analyzed). The number of iterations was 3. The following standards were used: carbon – $CaCO_3$; oxygen – SiO_2; titanium – Ti. The size of TiO_2 nanoparticles is shown in Fig. 6. The size of TiO_2 nanoparticles was shown to range from 70 – 90 nm.

TABLE 1. Date derived from EDAX

Element	Weight%	Atomic%
O K	9.03	22.90
Ti K	90.97	77.10
Totals	100.00	

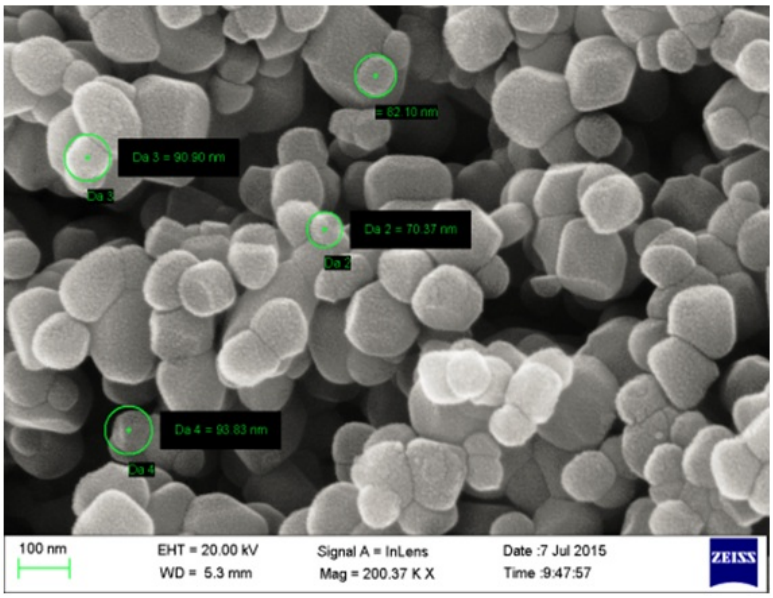

FIG. 3. The SEM image of TiO_2 nanoparticles

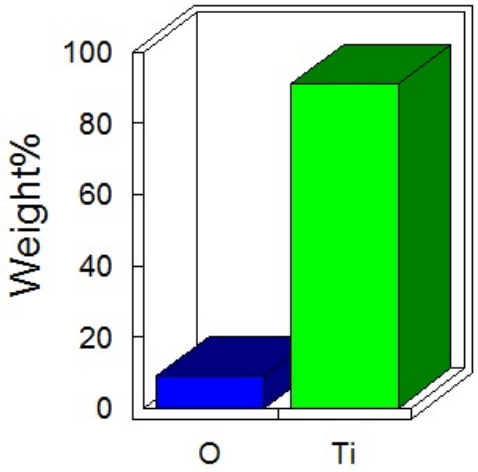

FIG. 4. The quantitative results of TiO_2 nanoparticles

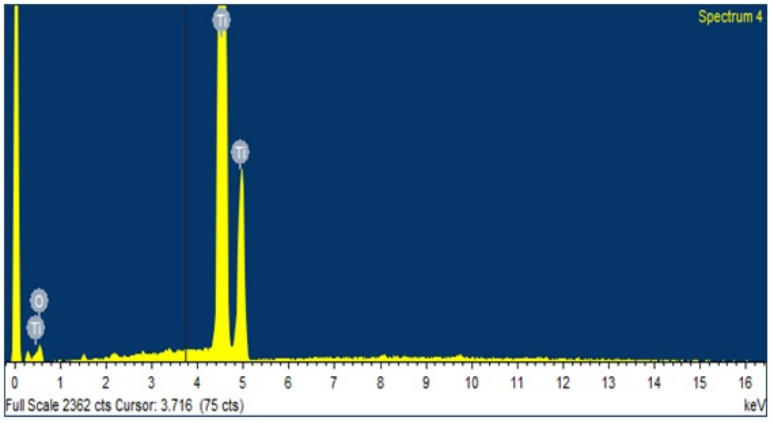

FIG. 5. EDAX spectrum of TiO_2 nanoparticles

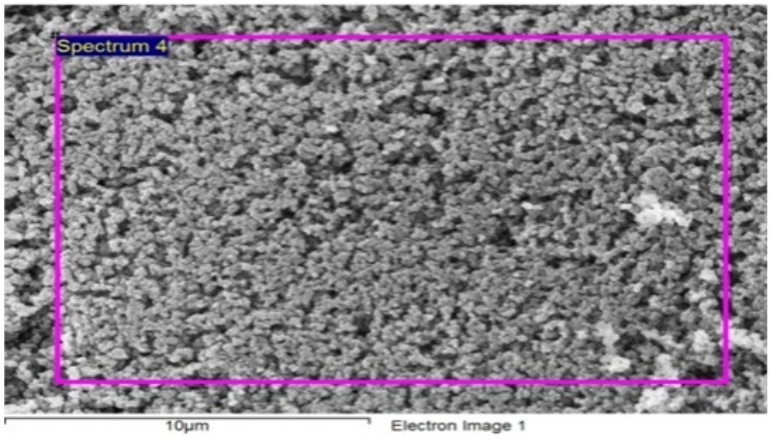

FIG. 6. The size of TiO_2 nanoparticles

4. Weight loss method

4.1. Corrosion inhibition by TiO_2 system

Corrosion rates (CR) of mild steel immersed in well water (WW) in the absence and presence of TiO_2 and the inhibition efficiencies (IE) obtained by weight loss method are given in Table 2. It was observed that when 100 ppm of TiO_2 was added to well water, the corrosion rate decreases to a great extent; and an inhibition efficiency of 80 % was obtained. This is due to the adsorption of TiO_2 nanoparticles on the metal's surface. As the concentration of TiO_2 increases, the corrosion rate decreases and the inhibition efficiency increases (Fig. 7) [17–20].

TABLE 2. Corrosion rates (CR) of mild steel immersed in well water (WW) in the absence and presence of TiO_2 and the inhibition efficiencies (IE) obtained by the weight loss method

TiO_2 Ppm	CR mdd	IE %
0	23.45	-
0	13.93	41
40	11.26	52
60	7.50	68
80	6.80	71
100	4.69	80

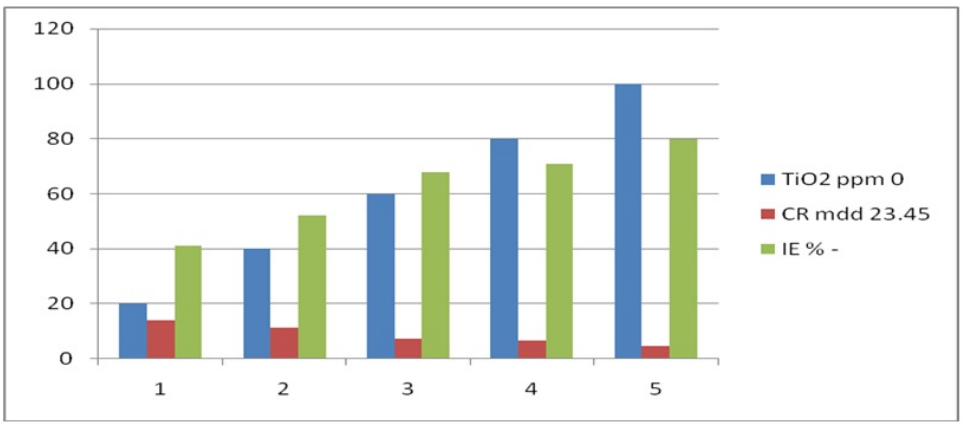

FIG. 7. Correlation between concentration of TiO_2, corrosion rate and inhibition efficiency

4.2. Corrosion inhibition by May flower extract (FE) system

Corrosion rates (CR) of mild steel immersed in well water (WW) in the absence and presence of May flower extract and the inhibition efficiencies (IE) obtained by weight loss method are given in Table 3. It was observed that when 10 ml of flower extract was added to well water, the corrosion rate decreases significantly and an inhibition efficiency of 84 % was obtained. This is due to the adsorption of active principles of May flower extract on the metal surface. As the concentration of flower extract increases, the corrosion rate decreases and the inhibition efficiency increases. (Fig. 8).

TABLE 3. Corrosion rates (CR) of mild steel immersed in well water (WW) in the absence and presence of May flower extract and the inhibition efficiencies (IE) obtained by weight loss method

FE ml	CR mdd	IE %
0	23.45	-
2	12.66	46
4	10.55	55
6	7.97	66
8	6.10	74
10	3.75	84

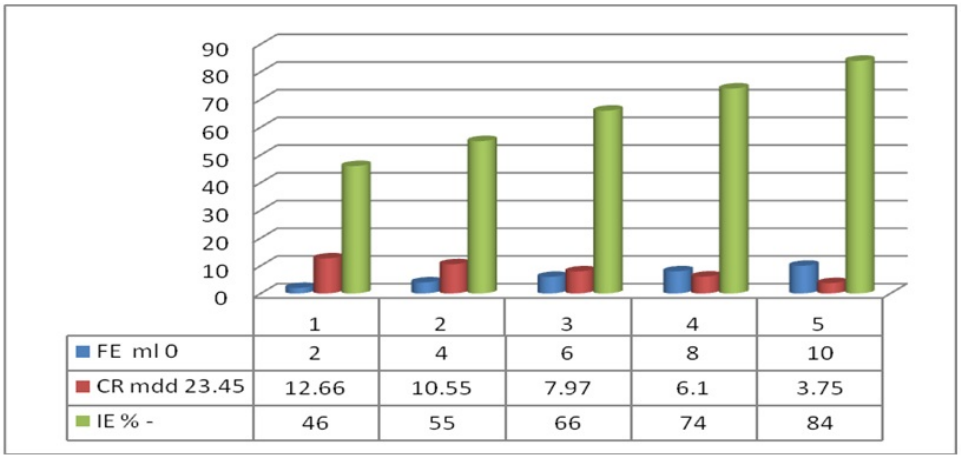

FIG. 8. Correlation between concentration of May flower extract, corrosion rate and Inhibition Efficiency (IE)

4.3. Corrosion inhibition by WW+ TiO_2 100 ppm + 10 ml of May FE System

Corrosion rates (CR) of mild steel immersed in well water (WW) in the absence and presence of TiO_2 and an aqueous extract of May flower extract (FE) and the inhibition efficiencies (IE) obtained by weight loss method are given in Table 4. It was observed that when 100 ppm of TiO_2 was added to well water, the corrosion rate significantly decreased, and an inhibition efficiency of 80 % was obtained. This is due to the adsorption of TiO_2 nanoparticles on the metal surface. When 10 ml of flower extract was added to well water, the corrosion inhibition efficiency was 84 %. When both 100 ppm of TiO_2 and 10 ml May flower extract were added, the IE was 95 %. Hence, one can conclude that the WW+ TiO_2 100 ppm + 10 ml of FE system offers the best inhibition efficiency. TiO_2 is adsorbed on the metal surface and offers corrosion protection by preventing water molecules and aggressive ions from reaching the metal surface. The active principles of FE are adsorbed on the TiO_2 layers. These layers are hydrophobic in nature and prevent water molecules reaching the metal surface (Fig. 9).

5. Adsorption isotherm for TiO_2 system

The adsorption of inhibitor molecules (TiO_2 ppm) obeys Langmuir Adsorption Isotherm (Fig. 10). A graph was made by plotting C vs C/θ, where C is concentration of inhibitor and θ is surface coverage. A linear plot

TABLE 4. Corrosion rates (CR) of mild steel immersed in well water (WW) in the absence and presence of TiO_2 and an aqueous May flower extract (FE) and the inhibition efficiencies (IE) obtained by weight loss method

System	CR mdd	IE %
WW	23.45	-
WW+$TiO_2$100 ppm	4.71	80
WW+10ml of FE	3.77	84
WW+$TiO_2$100 ppm + 10ml of FE	1.18	95

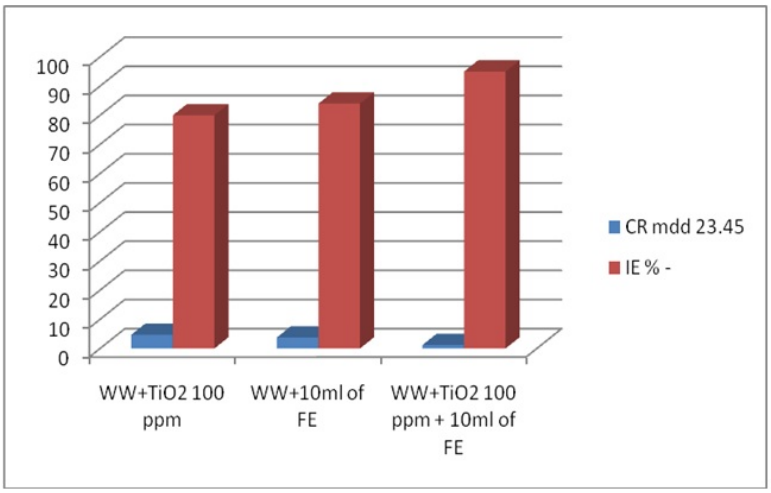

FIG. 9. Correlation between corrosion rates and inhibition efficiencies for various systems

was obtained with R^2 value of 0.980. This indicated that the adsorption of molecules on the metal surface obeyed the Langmuir adsorption isotherm. The slope was 0.940 and intercept was 33.88. The Langmuir constant, K (calculated from the relation Intercept = log K), was found to be 7.59×10^{33}.

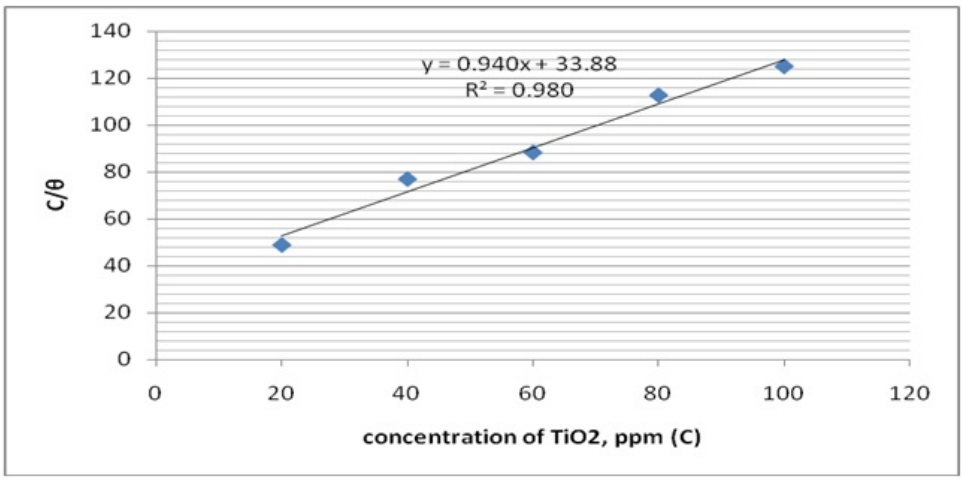

FIG. 10. Langmuir adsorption isotherm for TiO_2 system

Since the Langmuir adsorption isotherm is obeyed, it implies that:

- The adsorption of a single adsorbate onto a series of equivalent sites on the surface of the solid.
- The surface containing the adsorbing sites is perfectly flat plane with no corrugations (assuming an homogeneous surface).

- The adsorbing molecule adsorbs into an immobile state.
- All sites are equivalent.
- Each site can hold at most one molecule of inhibitor (monolayer coverage only).
- There are no interactions between adsorbed molecules on adjacent sites.
- The formation of Langmuir monolayers by adsorption onto a surface dramatically reduces the entropy of the molecular system

5.1. Adsorption isotherm for May flower system

The adsorption of inhibitor molecules (May flower extract in ml) obey Langmuir Adsorption Isotherm (Fig. 11). A graph was made by plotting C vs C/θ, where C is concentration of inhibitor and θ is surface coverage. A linear plot was obtained with R^2 value of 0.970. This indicated that the adsorption of molecules on the metal surface obeyed the Langmuir adsorption isotherm. The slope was 0.933 and the intercept was 3.088. The Langmuir constant, K (calculated from the relation Intercept = log K) was found to be 1225×10^3.

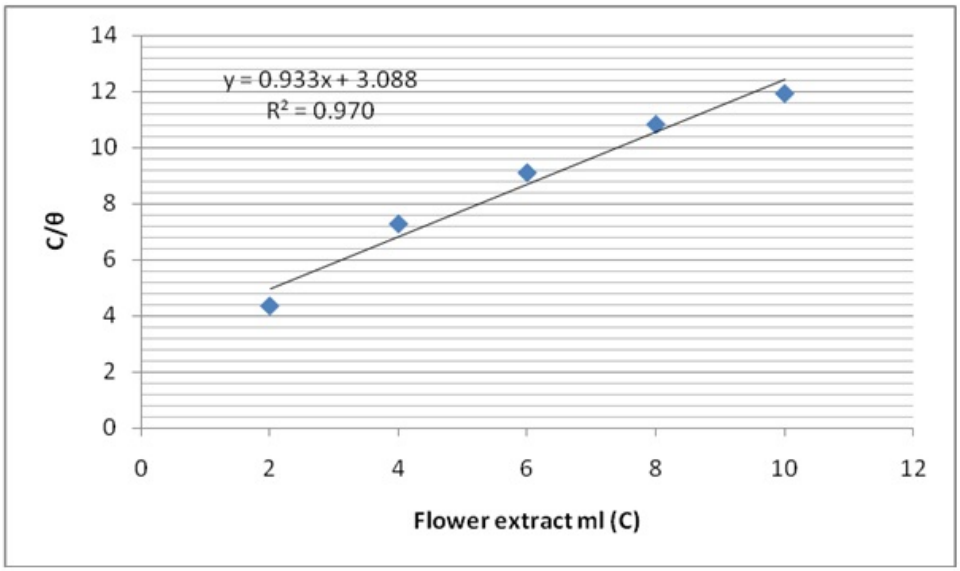

FIG. 11. Langmuir adsorption isotherm for May flower system

6. Potentiodynamic polarization study

Electrochemical analyses, such as Polarization study and AC impedance spectra, have been used to investigate the corrosion resistance of metals [20–25].

In the polarization study, if corrosion resistance increases, linear polarization Resistance (LPR) value increases and corrosion current decreases. In the present study, the corrosion resistance of mild steel immersed in well water in the presence and absence of an aqueous May flower extract and TiO_2 has been investigated by a potentiodynamic polarization study (Fig. 12). The corrosion parameters such as corrosion potential (Ecorr), Tafel slopes (bc = cathodic, ba = anodic), LPR values and corrosion current (Icorr), derived from the TAFEL plots, are given in the Table 5.

When mild steel was immersed in well water (WW), the corrosion potential was -631 mV vs SCE, the LPR value was 7249 ohm cm^2 and the corrosion current was 5.268×10^{-6} A/cm^2.

It is interesting to note that when mild steel was immersed in well water containing 100 ppm of TiO_2, the corrosion resistance of mild steel increased. This was due to the presence of TiO_2 nanoparticles in the medium. The nanoparticles were adsorbed onto the metal surface, forming a protective film. Hence, corrosion resistance increased. This was revealed by the fact that when the mild steel was immersed in WW containing TiO_2, the LPR value increased from 7249 ohm cm^2 to 8350 ohm cm^2. The corrosion current value decreased from 5.268×10^{-6} A/cm^2 to 1.587×10^{-6} A/cm^2.

When mild steel was immersed in WW+10 ml of FE + system, it was inferred that the corrosion resistance of mild steel increased. This was revealed by the fact that, in presence of flower extract, the LPR value was high (30994 ohm cm^2); the corrosion current decreased to 1.045×10^{-6} A/cm^2 and the corrosion potential shifted

TABLE 5. Corrosion parameters of mild steel immersed in well water (WW) in the absence and presence of TiO_2 and an aqueous flower extract (FE), obtained by polarization study

System	E_{corr} mV vs SCE	b_c mV/decade	b_a mV/decade	LPR ohm cm^2	I_{corr} A/cm^2
WW	−631	202	155	7249	5.268×10^{-6}
WW+TiO_2 100 ppm	−663	221	120	8350	1.587×10^{-6}
WW+10 ml of FE	−670	199	119	30994	1.045×10^{-6}
WW+TiO_2 100 ppm + 10 ml of FE	−641	186	165	36770	1.035×10^{-6}

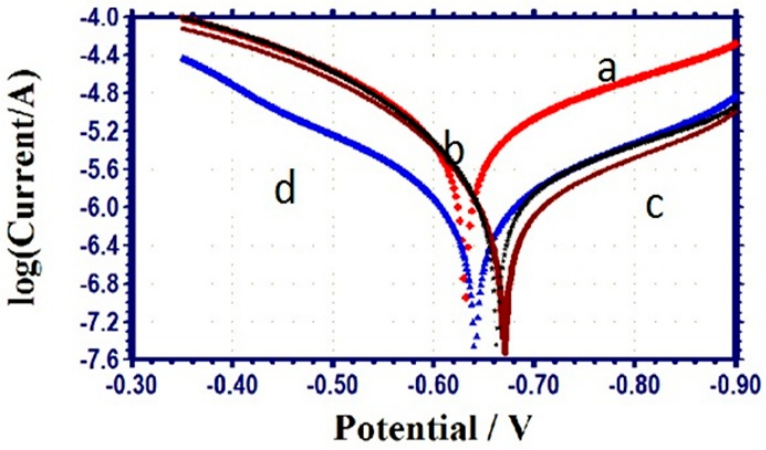

FIG. 12. Polarization curves of mild steel immersed in various test solutions (a) WW, (b) WW+TiO_2 100 ppm, (c) WW+10 ml of FE, (d) WW+TiO_2 100 ppm + 10 ml of FE

to the cathodic side (from −631 to −641 mV vs SCE). This means that the cathodic reaction was controlled predominantly. The active principle present in the flower extract forms a protective film on the metal surface. The transfer of electrons from the metal to the bulk of the system was prevented. Because of the necessity of electrons, the cathodic reaction, which involves the interaction of electrons with oxygen and water, is minimized, thus, the formation of hydroxide ions is reduced.

When mild steel was immersed in theWW+10 ml of FE + TiO_2 100 ppm system, the corrosion resistance of mild steel further appeared to be further increased. This is revealed by the fact that, in presence of flower extract, the LPR value was very high (36770 ohm cm^2); the corrosion current decreased to 1.035×10^{-6} A/cm^2 and the corrosion potential shifted to the cathodic side (from −631 to −670 mV vs SCE). This means that the cathodic reaction was controlled predominantly. The active principle present in the May flower extract forms a protective film on the metal surface. The transfer of electrons from the metal to the bulk of the system was prevented. Because of the need for electrons, the cathodic reaction, which involves the interaction of electrons with oxygen and water, is limited, thus, the formation of hydroxide ions is reduced. However, when compared with the WW+10 ml of FE system, (−670 mV vs SCE), the shift is anodic (−641 mV vs SCE). This shift revealed that in presence of TiO_2, the anodic reaction is also controlled. Moreover, when compared with −631 mV vs SCE, this shift is very small. So it can be considered that the "WW+10 ml of FE + TiO_2 100 ppm system" functions as a mixed inhibitor system, controlling both the anodic and cathodic reactions. **Thus, the polarization study leads one to the conclusion that the corrosion resistance of mild steel in various test solutions decreases in the order:**

WW+$TiO_2$100 ppm+10 ml of FE system>WW+10 ml of FE>WW+$TiO_2$100 ppm>WW

From the data, one can conclude that the WW+$TiO_2$100 ppm + 10ml of FE system offers better inhibition efficiency than other systems.

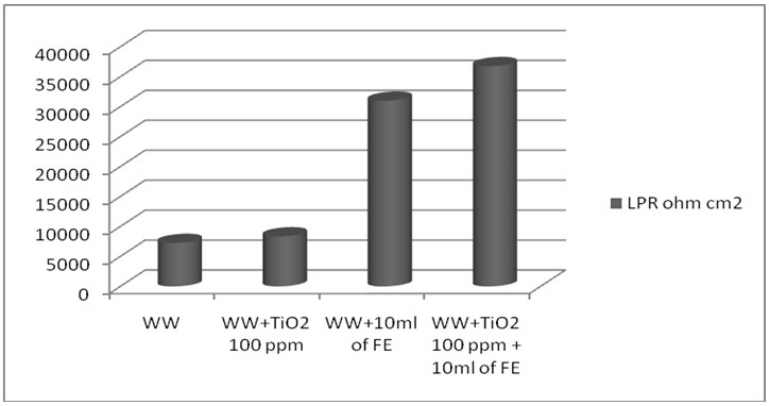

FIG. 13. Comparison of LPR values of various systems

6.1. AC impedance spectra

AC impedance spectra have been used to investigate the corrosion resistance of metals. When corrosion resistance increases, the charge transfer resistance values (R_t) increase, impedance values increase and double layer capacitance values (c_{dl}) decrease [26–30]. AC impedance spectra of mild steel immersed in various test solution are shown in Figs. 14 – 17. Nyquist plots are shown in (Fig. 14), and Bode plots are shown in Fig. 15 – 17. The corrosion parameters are given in Table 6.

TABLE 6. Corrosion parameters of mild steel immersed in well water (WW) in the absence and presence of TiO_2 and an aqueous May flower extract (FE), obtained by AC impedance spectra

System	R_t ohm cm^2	C_{dl} F/cm^2	Impedance Log(z/ohm)
WW	181	2.78×10^{-8}	2.543
WW+$TiO_2$100 ppm	782	0.639×10^{-8}	3.152
WW+10 ml of FE	1021	0.490×10^{-8}	3.251
WW+$TiO_2$100 ppm + 10 ml of FE	1080	0.463×10^{-8}	3.261

It was observed from Table 6 that when the inhibitor (TiO_2 100 ppm) was added to well water, the charge transfer resistance ($R_{t)}$ increased from 181 Ω cm^2 to 782 Ω cm^2. The C_{dl} value decreased from 2.78×10^{-8} F/cm^2 to 0.639×10^{-8} F/cm^2 and the impedance value increased from 2.543 to 3.152. These results lead one to conclude that a protective film was formed on the metal surface. Nanoparticles of TiO_2 have adsorbed on the metal surface forming protective film. The surface becomes hydrophobic, hindering water molecules and aggressive ions from reaching the surface, thus protecting the metal from corrosion.

When the inhibitor (10 ml of may flower extract) was added to well water, the charge transfer resistance (R_t) increased from 181Ω cm^2 to 1021 Ω cm^2, the C_{dl} value decreased from 2.78×10^{-8}F/cm^2 to 0.490×10^{-8} F/cm^2 and the impedance value increased from 2.543 to 3.251. These results would seem to indicate that a protective film was formed on the metal surface. This film is more compact and hydrophobic than the previous case, which is why the R_t value of this system is higher than that of the previous system.

It was observed that the WW+$TiO_2$100 ppm + 10 ml of FE system is more corrosion resistant than the previous system because for this system, the R_t value increases to 1080 Ω cm^2 and the C_{dl} value decreases to 0.463×10^{-8} F/cm^2 and the impedance value increases to 3.261. It seems that the flower extract and TiO_2 particles are adsorbed jointly on the metal surface and thus form a better protective film. Thus, AC impedance spectra lead to the conclusion that corrosion resistance of mild steel in various test solutions decreases in the following order:

WW+TiO_2 100 ppm+10 ml of FE system>WW+10 ml of FE>WW+TiO_2 100 ppm>WW.

The WW+TiO_2 100 ppm + 10 ml of FE system offers better inhibition efficiency than other systems. This view is in agreement with the polarization study results.

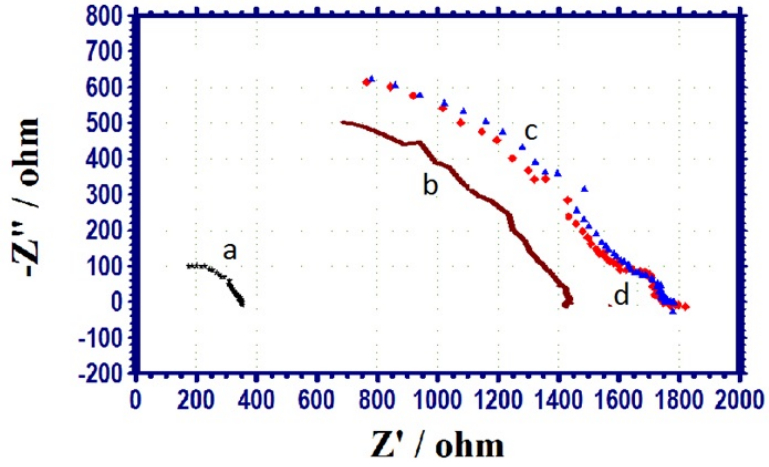

FIG. 14. AC impedance spectra (Nyquist Plots) of mild steel immersed in various test solutions (a) WW, (b) WW+TiO_2 100 ppm, (c) WW+10 ml of FE, (d) WW+TiO_2 100 ppm + 10 ml of FE

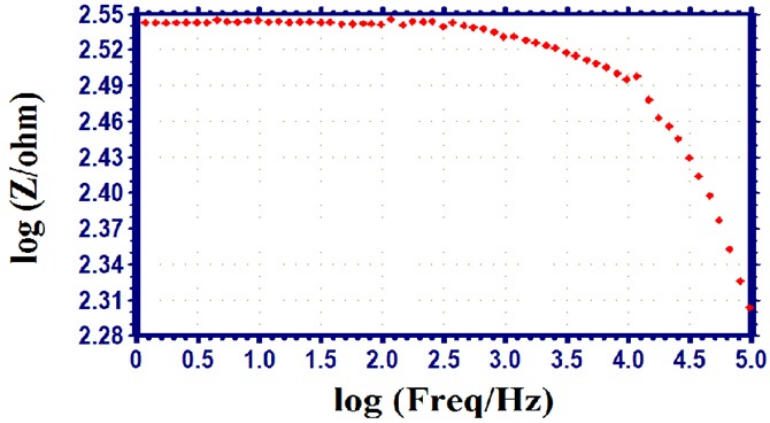

FIG. 15. AC impedance spectrum (Bode Plot- impedance) of mild steel immersed in well water (a) WW

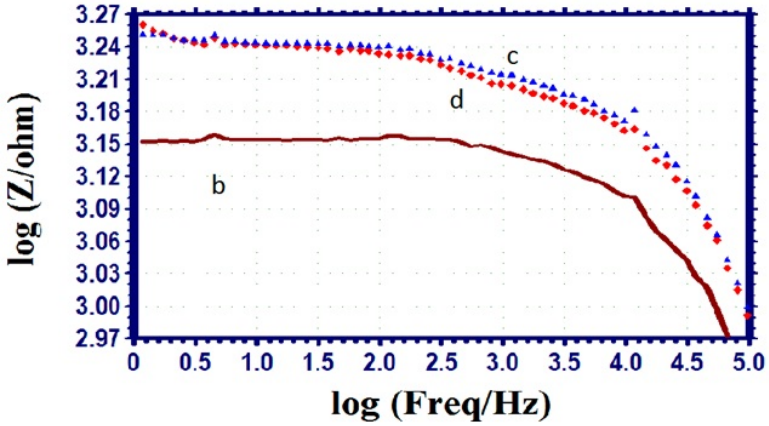

FIG. 16. AC impedance spectra (Bode Plots-impedance) of mild steel immersed in various test-solutions (b) WW+TiO_2 100 ppm, (c) WW+10 ml of FE, (d) WW+TiO_2 100 ppm + 10 ml of FE

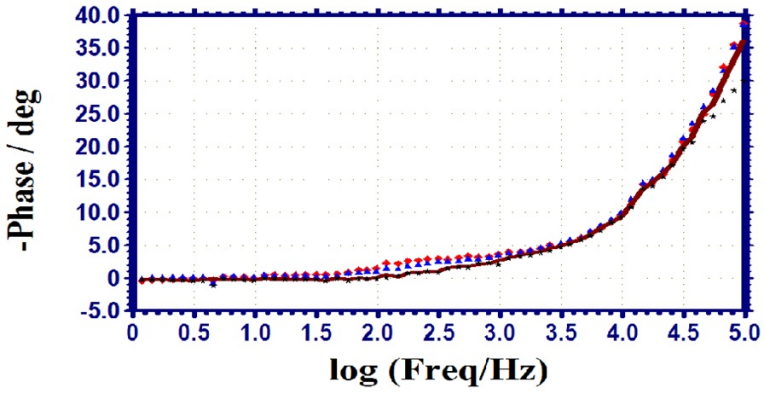

FIG. 17. AC impedance spectra (Bode Plots-phase angle) of mild steel immersed in various test Solutions. black line – WW, grey line – WW+ TiO_2 100 ppm, blue line – WW+ 10 ml of FE, red line – WW+TiO_2 100 ppm + 10 ml of FE

7. Conclusion

The present study leads to the following conclusions:

- Titanium dioxide nanoparticles, along with an aqueous may flower extract has been synthesized successfully.
- The formulation consisting of 100 ppm of TiO_2 nanoparticles and 10 ml may flower extract afforded a 95 % IE for mild steel immersed in well water.
- Polarization study reveals that 100 ppm of TiO_2 nanoparticles and 10 ml may flower extract functions as mixed inhibitor system, controlling both anodic and cathodic reactions.
- AC impedance spectra reveal that the formation of protective film on the metal's surface.

Acknowledgement

The authors are thankful to their respective management and Defence Research and Development Organisation, New Delhi.

References

[1] Lee H.J., Yeo S.Y., Jeong S.H. Antribacterial effect of nanosized silver colloidal solution on textile fabrics. *J. Master. Sci*, 2003, **38**, P. 219–2204.
[2] Alimohammadi F. *Stabilization of silver nanoparticles and antibacterial characterization on the cotton surface against washing*. M.Sc Thesis, Islamic Azad University Tehran South Brach, 2009.
[3] Aiken J.D., Finke R.G. A review of modern transition-metal nanoclusters: their synthesis, characterization, and applications in catalysis. *J. Mol. Catal, A:Chem*, 1999, **145**, P. 1–44.
[4] Liu R., Chen H., Hu S. Synthesis and characterization of nanometals with coreshell structure. *China Particuol*, 2004, **2**(4), P. 160–163.
[5] Sung-Suh H.M., Choi J.R., Hah H.J., Koo S.M., Bae Y.C. Comparison of Ag deposition effects on the photo catalytic activity of nanoparticle TiO_2, under visible and UV light irradiation. *J. Photochem. Photobiol. A*., 2004, **163**, P. 37–44.
[6] Valentine Rupa A., Manikandan D., Divaker D., Sivakumar T. Effect of deposition of Ag on TiO_2 nanoparticles on the photodegradation of Reactive Yellow-17. *J. Hazard, Mater.*, 2007, **147**, P. 906–913.
[7] Uddin M.J., Cesano F., Scarano D., Bonino F., Agostini G., Spoto G., Bordiga S., Zecchina A. Cotton textile fibers coated by Au/TiO_2 films: Synthesis characterization and self-cleaning properties. *J. Photochem. Photobiol. A.*, 2008, **199**, P. 64–72.
[8] Sclafant A., Herrmann J.M. Influence of metallic silver and of platinum-silver bimetallic deposits on the photocatalytic activity of titania (anatase and rutile) inorganic and aqueous media. *J. Photochem. Photobiol. A.*, 1998, **113**, P. 181–188.
[9] Deyab M.A., Keera S.T. Effect of nano-TiO_2 particles size on the corrosion resistance of alkyl coating. *Chemistry and Physics*, 2014, **146**(3), P. 406–411.
[10] Kim K.M., Lee E.H., Hur D.H. Corrosion behavior on Ni-base alloys applied with Nano-TiO_2 in high temperature caustic water. *Current Nanoscience*, 2014, **10**(1), P. 89–93.
[11] Liu T., Qiang L. Research on inhibition marine microbial adherence of a novel nano-TiO_2 coating on aluminium. *Advanced Materials Research*, 2012, **557-559**, P. 1687–1690.
[12] Sakata T., Kawai T., Hashimoto K. Catalytic Properties of Ruthenium Oxide on n-Type Semi-conductors under Illumination. *J. Phys. Chem.*, 1984, **88**, P. 2344–2350.
[13] Fu X.Z., Zeltner W.A., Anderson M.A. Photocatalytic Generation of H_2 from Seawater. *Appl. Catal.,* 1995, **B6**, P. 209–220.
[14] Sopyan I., Watanabe M., Murasawa S., Hashimoto K., Fujishima A. A film-type photocatalyst incorporating highly active TiO_2 powder and fluororesin binder: photocatalytic activity and long-term stability. *J. Electroanal. Chem.*, 1996, **415**, P. 183–186.

[15] Zhang X., Fujishima A., Alexei M.J., Emeline V. Murakami T. Double-Layered TiO_2-SiO_2. Nanostructured Films with Self-Cleaning and Antireflective Properties. *J.Phys Chem*, 2006, **B110**, P. 25142–25148.
[16] Zhou et al. Titanium dioxide nanoparticles and nanoparticle suspensions and methods of making the same. US Patent 7326399 B2, 2008.
[17] Hansoon C.M. Volume Relationship for C-S-H Formation Based on General Concepts. *Cem. Concr. Res*, 1984, **14**, P. 574.
[18] Nakayama N., Obuchi A. Inhibitory effects of 5-aminouracil on cathodic reactions of steels in saturated $Ca(OH)_2$ solution. *Corros. Sci.*, 2003, **45**, P. 2075–2092.
[19] Manivannan M., Rajendran S. Investcation of inhibitive action of urea-Zn^{2+} system in the corrosion control of carbon steel in sea water. *International of Engineering science and Technology*, 2011, **3**, P. 19–23.
[20] Johnsirani V., Sathiyabama J., Rajendran S, Shanthi T., Muthumegala T.S., Krishnaveni A. Inhibitive action of malachite green-Zn^{2+} system. *Bulgarian Chemical Communication*, 2012, **44**, P. 41–51.
[21] Epshiba R., Peter Pascal Regis A., Rajendran S. Inhibition Of Corrosion Of Carbon Steel In A Well Water By Sodium Molybdate – Zn^{2+} System. *Int. J. Nano. Corr. Sci. Engg.*, 2014, **1**(1), P. 1–11.
[22] Kavitha N., Manjula P. Corrosion Inhibition of Water Hyacinth Leaves, Zn^{2+} and TSC on Mild Steel in neutral aqueous medium. *Int. J. Nano. Corr. Sci. Engg.*, 2014, **1**(1), P. 31–38.
[23] Nagalakshmi R., Nagarajan L., Joseph Rathish R., Santhana Prabha S., Vijaya N., Jeyasundari J., Rajendran S. Corrosion Resistance of SS316l In Artificial Urine In Presence Of D-Glucose. *Int. J. Nano. Corr. Sci. Engg.*, 2014, **1**(1), P. 39–49.
[24] Angelin Thangakani J., Rajendran S., Sathiabama J., M.Joany R. Joseph Rathis R., Santhana Prabha S. Inhibition of Corrosion of Carbon Steel In Aqueous Solution Containing Low Chloride Ion By Glycine – Zn^{2+} System. *Int. J. Nano. Corr. Sci. Engg.*, 2014, **1**(1), P. 50-62.
[25] Nithya A., Shanthy P., Vijaya NJoseph Rathish. R., Santhana Prabha S., Joany R.M., Rajendran S. Inhibition of Corrosion of Aluminium By An Aqueous Extract of Beetroot (Betanin), *Int. J. Nano Corr. Sci. Engg.*, 2015, **2**(1), P. 1–11.
[26] Gowrani T., Manjula P., Nirmala Baby C. Manonmani, Sudha K.N., Vennila R. Thermodynamical Analysis of MBTA on The Corrosion Inhibition of Brass In 3 % NaCl Medium. *Int. J. Nano. Corr. Sci. Engg.*, 2015, **2**(1), P. 12–21.
[27] Namita K., Johar K., Bhrara R., Epshiba R., Singh G. Effect Of Polyethoxyethylene N, N, N‘ 1, 3 Diamino Propane on The Corrosion of Mild Steel In Acidic Solutions. *Int. J. Nano Corr. Sci. Engg.*, 2015, **2**(1), P. 22–31.
[28] Christy Catherine Mary A., Rajendran S., Hameed Al-Hashem, Joseph Rathish R., Umasankareswari T., Jeyasundari J. Corrosion Resistance Of Mild Steel In Simulated Produced Water In Presence Of Sodium Potassium Tartrate. *Int. J. Nano Corr. Sci. Engg.*, 2015, **2**(1), P. 42–50.
[29] Sangeetha M.,Rajendran S., Sathiyabama J., Umasankareswari T., Krishnaveni A., Joany R.M., *Int. J. Nano. Corr. Sci. Engg*, 2015, **2**(3), P. 14–21.
[30] Nithya Devi P., Sathiyabama J., Rajendran S. Joseph Rathish R., Santhana Prabha S. Influence of citric acid-Zn^{2+} System on Inhibition of Corrosion of Mild Steel in Simulated Concrete Pore Solution. *Int. J. Nano Corr. Sci. Engg.*, 2015, **2**(3), P. 1–13.